EVALUATION OF FARADAY-SHIELDED STIX COILS FOR ION CYCLOTRON RESONANCE HEATING OF A PLASMA

by

N. B. Dodge

Magne Kristiansen

Arwin A. Dougal

April 30, 1966

Technical Report No. 3 on National Aeronautics and Space Administration
Grant NsG-353
"Propagation and Dispersion of Hydromagnetic and Ion Cyclotron Waves in Plasmas Immersed in Magnetic Fields"

Electrophysics Research Division
Attn: Dr. Harry Harrison, Chief, and I. R. Schwartz
Office of Grants and Research Contracts, Code SC
National Aeronautics and Space Administration
Washington, D. C. 20546

PLASMA DYNAMICS RESEARCH LABORATORY
DEPARTMENT OF ELECTRICAL ENGINEERING
THE UNIVERSITY OF TEXAS
AUSTIN, TEXAS 78712

Faculty Member Initiator and Principal Investigator:
Dr. Arwin A. Dougal
Professor of Electrical Engineering

ABSTRACT

The spatial waveform of the azimuthal electric field (E_θ) of the Stix coil is investigated. Methods are developed to improve the E_θ waveform by making it more nearly sinusoidal. Varying the spacing between individual coil turns in the coil section, along with the use of a "squirrel-cage" type Faraday shield are found to give a more nearly sinusoidal waveform. The effect of a number of Faraday shields on the E_θ waveform is also presented and it is found that certain types of shields, notably the single-slit copper cylinder shield, introduce distortions into the accelerating (E_θ) field. The efficiency of these shields in reducing the longitudinal electric field (E_z) is reported. Several are found to be efficient E_z shields, except for a Faraday shield placed outside the Stix coil. The effect of Faraday shields on the equivalent circuit parameters of the Stix coil is also determined and the variation of these parameters among the various shields is tabulated.

Author

TABLE OF CONTENTS

LIST OF FIGURES

LIST OF TABLES

CHAPTER I

INTRODUCTION

Of the many processes of direct energy conversion being studied today, none has more promise for the future of mankind than thermonuclear fusion. The reward for mastery of this process, unlimited energy at the disposal of our civilization, seems much nearer today than ever before, and a number of methods for achieving thermonuclear fusion are being studied throughout the world.

Ion cyclotron resonance heating (ICRH) offers one such promising method for eventually heating the ion constituents of a plasma to thermonuclear temperatures. Heating is accomplished by accelerating the ions at their natural frequency of oscillation in a magnetic field,[1,2,3] the accelerating mechanism being either the time-varying radial or azimuthal component (in cylindrical geometry) of an electric field whose frequency is at or near the natural(cyclotron) frequency of the ions. One device that has been widely used as the accelerator or energy coupler for ICRH is the Stix coil,[1,4] shown in Fig. I-1a (which imposes an E_θ accelerating field) although other methods of energy coupling have been proposed and used.[5,6,7]

In addition to the E_θ component, the Stix coil also introduces a z-component of electric field, due to the potential difference between adjacent coil turns. This "fringing" E_z is harmful to the energy coupling mechanism because interaction of the plasma and E_z field results in forces which drive energetic particles into the walls of the plasma container, releasing impurities that contaminate and cool the plasma. In order to "short out" or reduce the E_z component of the field, a Faraday shield has been employed. Usually this shield consists of a coaxial conductor or group of conductors placed between the Stix coil and the plasma, parallel to the axis of the plasma column.

Research on the ICRH experiment at The University of Texas indicated the need for an investigation of the Stix coil and Faraday shield, which are employed on this experiment, both separately and as a unit. Several questions

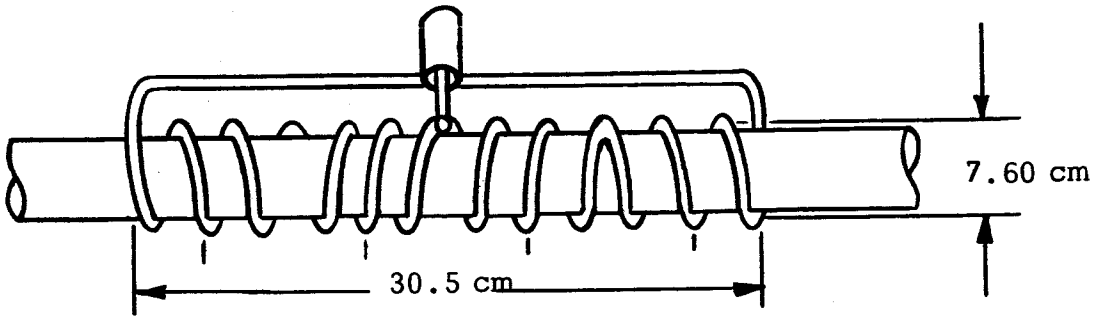

Fig. I-1a Two-Wavelength Stix Coil

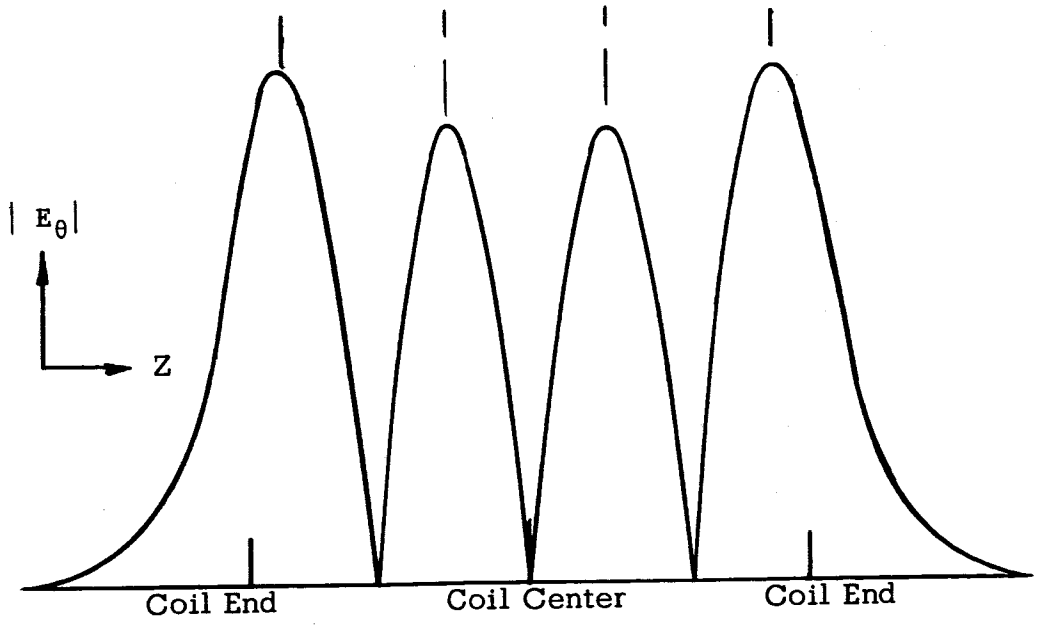

Fig. I-1b $|E_\theta|$ Field Associated with Stix Coil of Fig. I-1a

arose from the use of Stix coil and Faraday shield which had not, to the satisfaction of those at this facility, been answered in the existing literature on the subject.

The Stix coil itself is usually treated theoretically as a current-sheet device, which it does not closely approximate under experimental conditions. Also, since it is shorter than the plasma column, end effects are introduced into the spatially-varying standing waveform created by the coil. These effects considerably distort the E_θ field imposed on the plasma so that part of the input energy is wasted.

Besides a concern for the shape of the E_θ field, there were questions as to the shielding efficiency of the Faraday shield. Also, a number of Faraday shields have been mentioned in the literature, and there had been no comparison made, to the author's knowledge, of these various shields. Finally, because of the inductive and capacitive coupling between coil and shield, the Faraday shield may cause excessive loading of the coil circuit, effectively increasing the equivalent circuit coil resistance. The loading effect of various shields had not at this time been studied, although there had been one investigation of a particular shield.[8]

The above considerations provided the primary motivation for this study. A test apparatus was constructed, separate from the ICRH facility to avoid any interferences with the basic experiments in ICRH, and for convenience in testing.

It was felt that the data from what was essentially a "vacuum-case" investigation was applicable to the plasma case, since the E_θ standing waveform created by the Stix coil and the E_z shielding or shorting effect of the Faraday shield, as well as its effect on the coil circuit parameters, were more or less completely independent from the plasma effects. It was recognized, of course, that the plasma-shield-coil interactions, which involve complex reactive coupling mechanisms, introduce further distortions which can only be studied in the plasma case on the actual experiment.

A number of modifications of the copper-tubing Stix coil were made, and several Faraday shields were constructed. The investigation was primarily

concerned with improving the E_θ field shape and E_z shielding, determining the distortion of the E_θ waveform due to the Faraday shields, and examining the change in the Stix coil equivalent circuit parameters due to the addition of the shields. Significant improvements in coil and shield performance were achieved as a result of these investigations.

CHAPTER II.

DISCUSSION OF STIX COIL AND FARADAY SHIELD

Early research in ICRH faced the problem of coupling energy into a plasma without creating excessive space charge. A number of methods were proposed to overcome this difficulty. The "Stix" coil suggested by T. H. Stix in 1958,[1,4] has been the most widely accepted energy coupling device. The phase-reversed windings of this coil tend to partially neutralize the space charges, and it has proven to be an effective coupler of waves to the plasma column at higher plasma densities.

However, as mentioned in the introduction, the Stix coil itself introduces distortions into the E_θ waveform. Fig. I-1b shows an $|E_\theta|$ waveform for the typical two-wavelength copper-tubing Stix coil of Fig. I-1a. The coil end effects cause the outer two lobes of the E_θ field to be larger, introducing spatial harmonic distortions. Also, further distortions are introduced by the gradual (rather than sinusoidal) decay of E_θ outside the end of the coil. This second end effect is particularly harmful in that it alters the fundamental wavelength as well as introducing considerable harmonic distortion. A similar increase in wavelength has also been reported elsewhere.[9]

The copper-tubing Stix coil, as mentioned above, is the most common type of coil. As shown in Fig. I-1a, the coil usually consists of four sections of turns in opposite directions to create several wavelengths (two, as shown in the figure). These wavelengths correspond approximately to the anticipated length of the actual travelling wave in the plasma. The number of turns per section may vary from one to four or five. Generally, it has been accepted that increasing the number of turns per coil section reduces the harmonic content somewhat,[10] although this is not as important as was previously thought, a fact to be discussed more thoroughly in the results section. However, since a constant wavelength is involved, increasing the number of turns per section narrows the spacing distance, which can result in arcing between adjacent turns at high coil voltages. This limits the number of turns practically, so that three or four turns per section has been determined to be the optimum for

the experiment at this facility. At present, a four section coil of four turns per section (4-4-4-4 coil) is employed on the main ICRH experiment. A 3-3-3-3 coil, which had previously been used on the main experiment, was used for most of the studies of Faraday shields. In order to investigate the relative importance of the number of turns per section, a 1-1-1-1 coil was built for comparison with the 3-3-3-3 coil. A 3-4-4-3 coil was also constructed to investigate the result of varying the turns ratio in individual sections, as discussed in the results.

The Faraday shield should combine two basic characteristics: a) the highest E_z shielding efficiency possible, and b) distorting the E_θ (accelerating) field as little as possible. In order to optimize these two conditions eight shields were constructed, the design of each shield being suggested by its use at this facility or by some reference in the literature:

S-1, a solid copper cylinder shield, 0.010" thick, with one slit approximately 5/8" wide parallel to the shield (Fig. II-1a),

S-2, a multi-strip shield made of 0.030" copper strips 3/8" wide spaced 3/8" apart (Fig. II-1b). (Identical to the shield on the main ICRH experiment),

S-3, a "squirrel-cage" shield of 0.030" copper strips 3/16" wide spaced 3/16" apart, with a shorting strap at each end connecting all strips together (Fig. II-1c),

S-4, a shield identical to S-3 except for larger diameter so that it could be fitted outside the coil,

S-5, S-6 shields identical with S-2 except that the width and thickness of the strips were varied,

S-7, a shield consisting of colloidal graphite solution ("Aquadag") painted on a mylar sheet,

S-8, a shield of resistive paper bonded to mylar backing.

All shields were insulated from the Stix coil by mylar sheets and each had a grounding strap (the "squirrel-cage" shields were grounded at both ends).

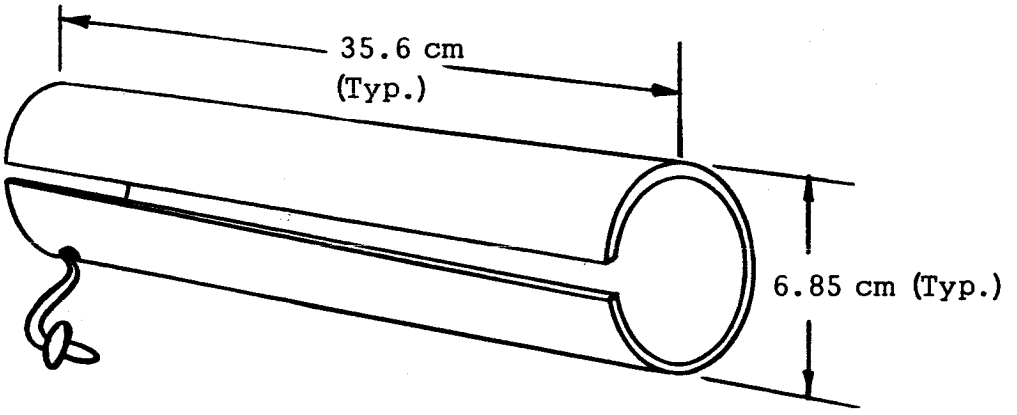

Fig. II-1a Single-Slit, Solid Copper Faraday Shield

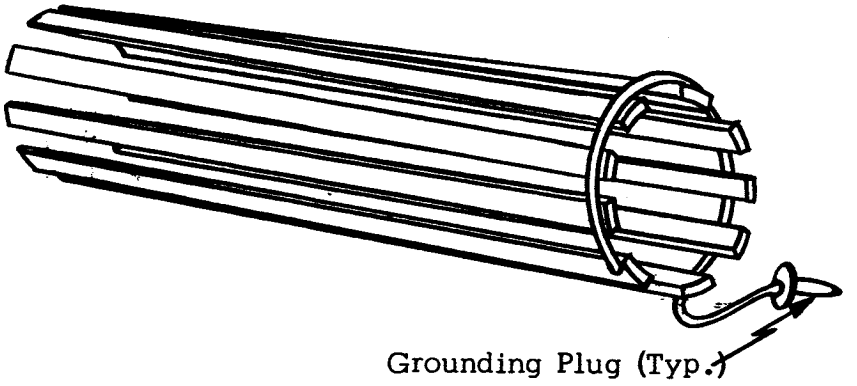

Fig. II-1b Multi-Strip Faraday Shield

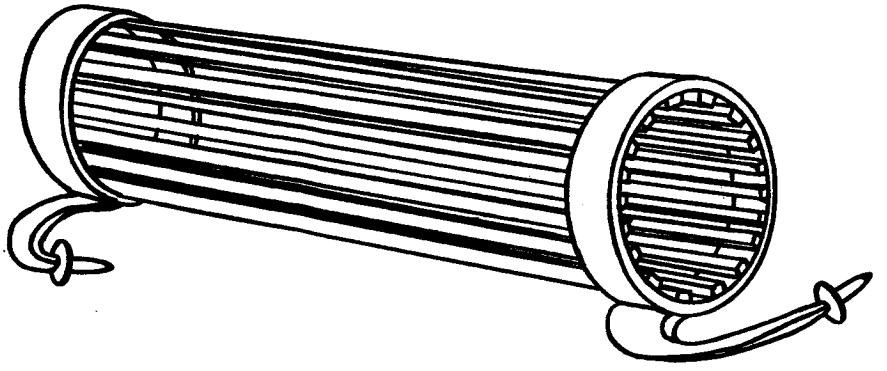

Fig. II-1c "Squirrel-Cage" Faraday Shield

CHAPTER III.

TRANSDUCER THEORY AND CONSTRUCTION

The field quantities of interest are E_θ and E_z. Transducers for both these quantities were required for the studies to be made. The E_θ probe was available, since such a probe has been used on the main ICRH experiment at The University of Texas.[11] This probe is a simple electromagnetic coil pickup, sensitive to the time rate of change of the axial (z) component of magnetic field ($\dot{B}_z$). The proportionality between E_θ and $\dot{B}_z$ can be developed as follows: Recall Maxwell's equation:

$$\nabla \times \vec{E} = -\partial\vec{B}/\partial t$$

This vector equation may be separated into three scalar equations. Examining the Z (axial) component in cylindrical coordinates:

$$(1/r)\partial(rE_\theta)/\partial r - (1/r)\partial E_r/\partial\theta = -\dot{B}_z$$

where $\quad (\dot{}) \equiv (\partial/\partial t)$

Now, E_r and its θ derivative will be very small compared to the other E components in the vacuum case, so that the third term may be neglected. Therefore:

$$\partial(rE_\theta)/\partial r = -r\dot{B}_z$$

$$d(rE_\theta) = -r\dot{B}_z dr$$

$$E_\theta = -(1/r)\int_o^r r'\dot{B}_z dr'$$

Integrating by parts:

$$(1/r)\int_o^r r'\dot{B}_z dr' = (1/r)[\,(r^2/2)\dot{B}_z - \int_o^r (r'^2/2)(\partial\dot{B}_z/\partial r')dr'$$

But $\quad \partial\dot{B}_z/\partial r = -(i\omega)\partial B_z/\partial r \simeq 0,$

since B_z is only a gradually varying function of r over the inner portion of the Stix coil. Therefore:

$$E_\theta = -(1/r)(r^2/2)\dot{B}_z = -(r/2)\dot{B}_z.$$

Hence, the coil pickup, oriented in a plane perpendicular to the coil axis, provides a direct indication of $| E_\theta |$. To provide preliminary verification of the above derivation, a number of plots were made by hand of $\dot{B}_z$ versus coil position, using a pickup coil from the main experiment, a Tektronix Model 555 oscilloscope for display, and a Boonton Model 160-A Q meter as a driving source for the 3-3-3-3 Stix coil. Such a plot is shown in Fig. III-1; it corresponded within experimental limits to a theoretical plot of E_θ.

Maxwell's equations provide no similar, simple, relationship for E_z. Two methods were developed to measure E_z. The first method utilized an electrostatic probe and a piece of conducting paper, the theory growing out of the relation of Stix coil and Faraday shield in the shielding process.

The Faraday shield is constructed so that E_z is affected primarily; E_θ is only negligibly affected (with one exception to be noted in the results section). In the vacuum case, E_r (the radial field component) does not exist, or is negligibly small. When a tube of conducting paper (carbon or graphite impregnated paper) is placed inside the Stix coil (or inside the Faraday shield, when it is in use), it will develop a potential proportional to the two field components. Since the Faraday shield primarily alters the E_z level, any change in the potential of the conducting paper between the unshielded and shielded conditions must be primarily due to a change in E_z. Thus, a method exists for qualitatively evaluating the shielding efficiency of the various shields.

Although the above method does give qualitative indications of the shielding efficiency, it is relatively inefficient and suffers from one great drawback; the potential on the paper conductor is more or less constant, the average over the entire length of the Stix coil. What is needed is a more reliable, quantitative picture of the shielding efficiency giving a picture of the spatial variation of E_z along the Stix coil. Subsequent to the development

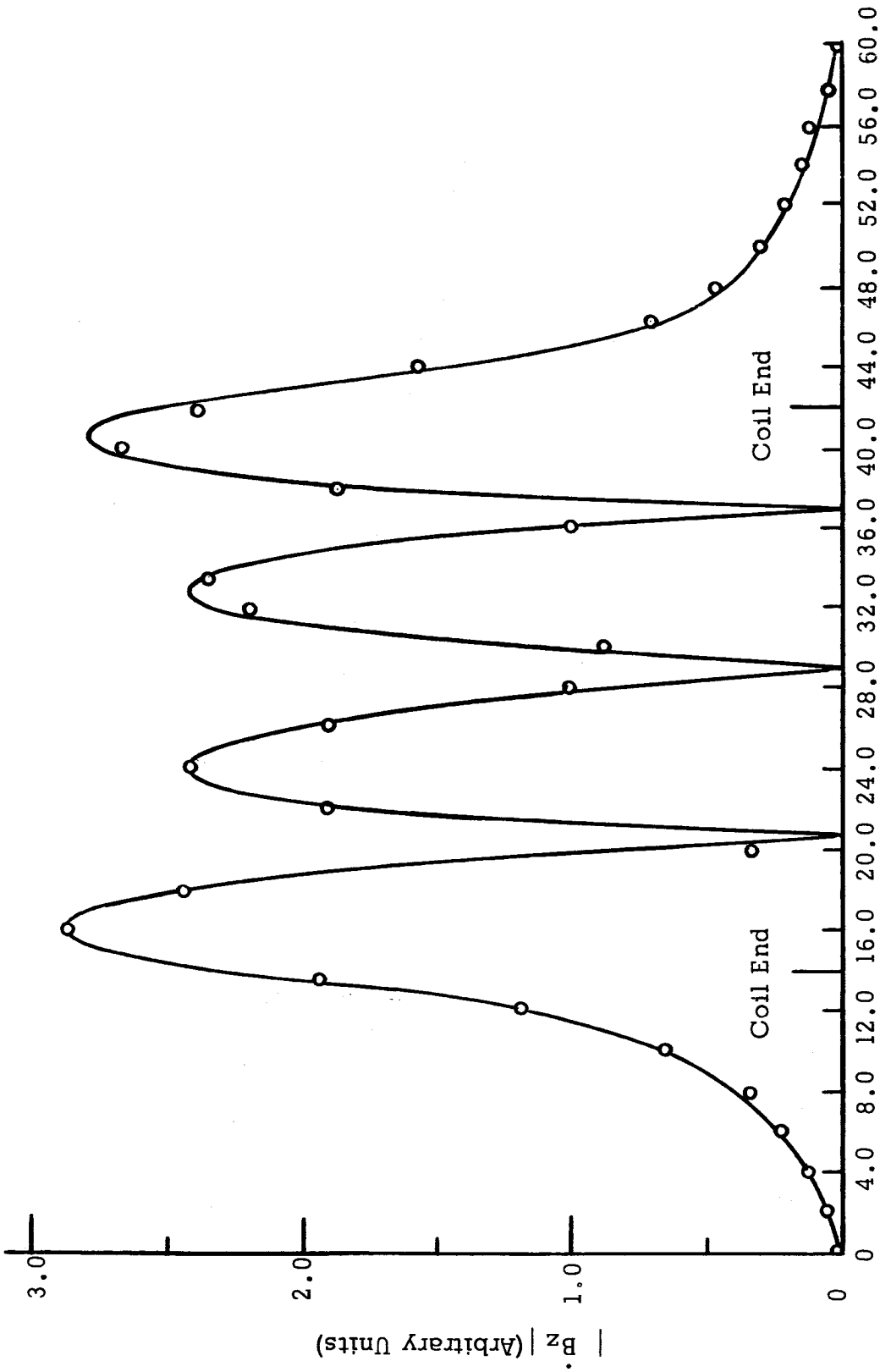

Fig. III-1 Preliminary Plot of $|\dot{B}_z|$ From Tabulated Values

of the potential probe, a dipole probe was developed which did provide the desired accuracy and spatial measurements.

The dipole probe is merely a small dipole antenna which couples to the E_z field and is oriented along the Stix coil axis (Fig. III-2a). Common mode signals coupled from the E_θ field may be eliminated by using a differential amplifier to amplify the probe signal.

The probes were constructed as follows:

The dipole E_z probe (Fig. III-2a) consists of two wires, inner conductors of solid coaxial cable. The lead-in to the dipole is an extension of the solid coaxial cable, the outer conductor providing shielding below the dipole. The solid coaxial cables are set in a phenolic tube for rigidity, and to enable clamping in the test apparatus discussed below. The cables are soldered to twin RG-174 lead-ins which are terminated in standard BNC connectors.

The $\dot{B}_z$ pickup (Fig. III-2b) is an 18-turn coil of #32 nylclad copper wire with the face of the coil such that when properly arranged on the experiment, the plane of the coil is perpendicular to the axis of the Stix coil. It is set in the end of a phenolic tube with an R G 58/U cable running through the tube to the coil, also terminated in a standard BNC male connector.

The electrostatic pickup (Fig. III-2c) is solid coaxial cable (copper tubing outer conductor), 1/8" O D , with the pickup the tip of the bared center conductor, polished with fine emery paper. The pickup is placed against the tube of conducting paper set inside the shield-coil arrangement, the potential registered by the probe being the signal sent to the diagnostic apparatus.

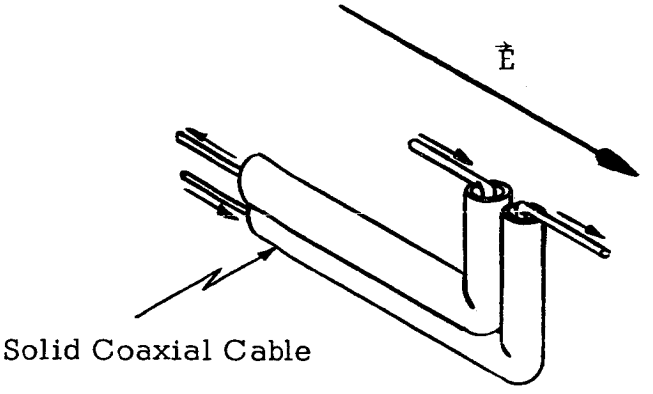

Fig. III-2a Dipole Probe Showing Current Induced by E_z Field of Polarity Shown in Figure

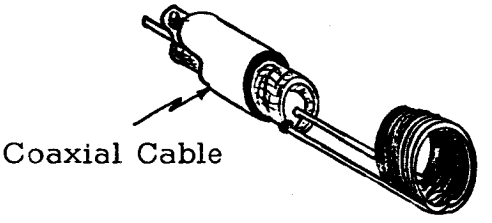

Fig. III-2b $\dot{B}_z$ (E_θ) Electromagnetic Probe

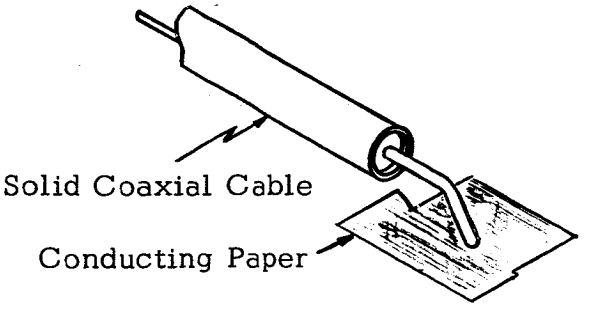

Fig. III-2c Electrostatic Probe

CHAPTER IV.

ELECTROMECHANICAL FIELD PLOTTER AND DIPOLE PROBE DIAGNOSTIC EQUIPMENT

In the preliminary work done verifying the $E_\theta - \dot{B}_z$ relationship and investigating the wave fields of the Stix coil, hand plotting of $|\dot{B}_z|$ versus axial position in the coil (z) proved to be tedious and time consuming. Since it was anticipated that a large number of curves of the field components for the numerous coil-shield combinations would be needed, it was soon obvious that an automatic plotting device was very desirable. Such a device would obtain two signals, one proportional to the transducer position in the coil, the other to the field component, which would then be fed to an automatic plotting device such as an X-Y recorder. Such an automatic plotter was constructed, and is described below.

The diagnostic equipment consists of the position transducers, $|\dot{B}_z|$ transducer coil, electrostatic pickup, dipole probe, amplifiers, voltmeters, and the X-Y recorder.

The $\dot{B}_z$ diagnostic apparatus is shown in Fig. IV-1. The Stix coil is supported in place on one end of an optical bench with a precision one meter scale graduated in millimeters and marked in centimeters. The transducers are placed in a holder consisting of a sliding support on the bench itself and standard laboratory clamps which are adjustable in the planes transverse to the coil axis.

To the base of the sliding support is attached a plastic bracket on which is mounted a metal contact clip, constructed so that a constant force is applied against a resistance wire, which runs the length of the optical bench. This resistance wire is a part of the position indicator (Fig. IV-2) which transmits the position of the transducer to the X-input of the recorder. The position indicator itself, as seen in the figure, is a simple bridge circuit utilizing two 1.5 volt batteries as a voltage source, which provides a dc signal proportional to the axial position of the pickup. The bridge circuit has been repeatedly

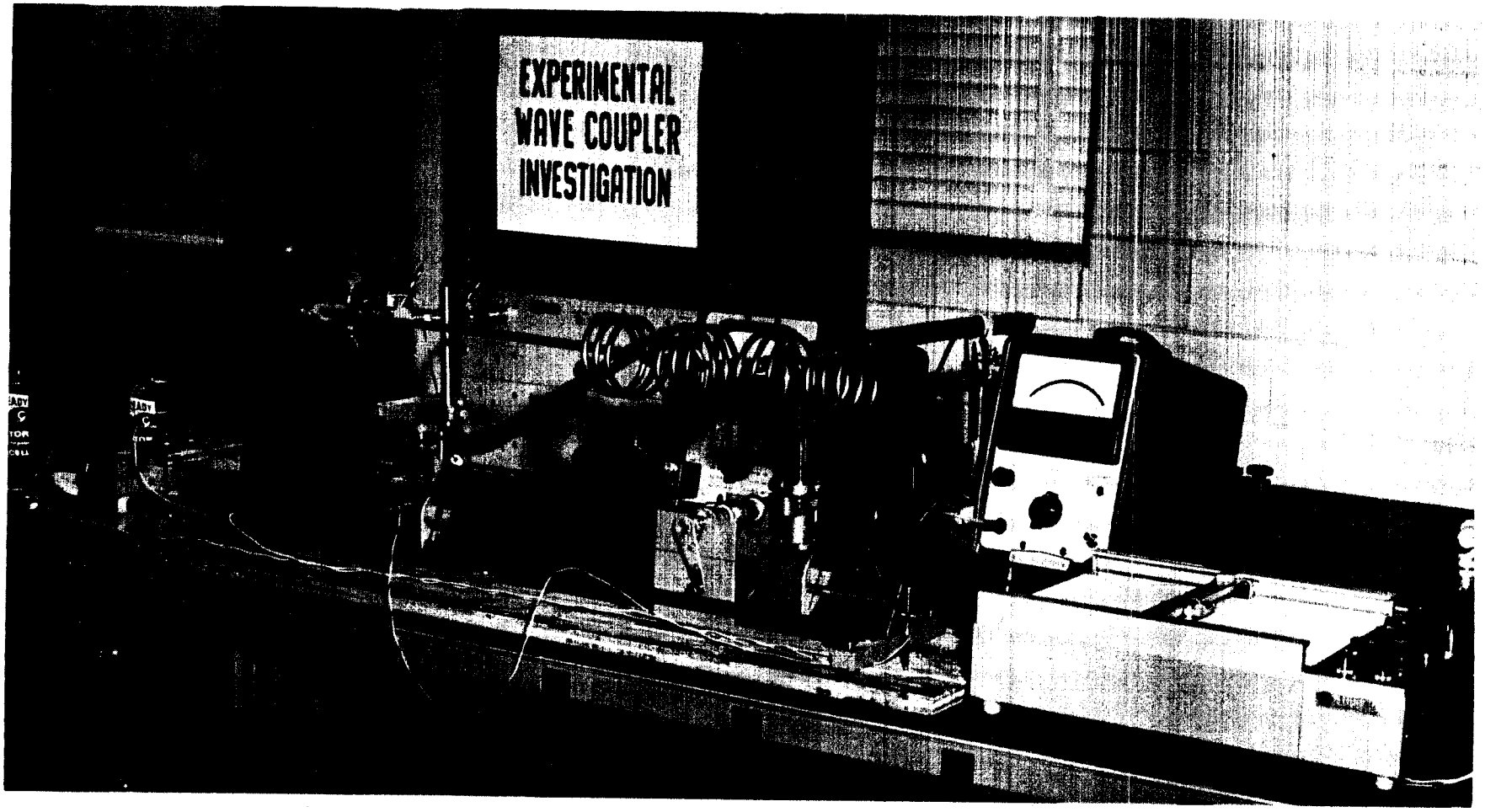

Fig. IV-1 Electromechanical Field Plotter

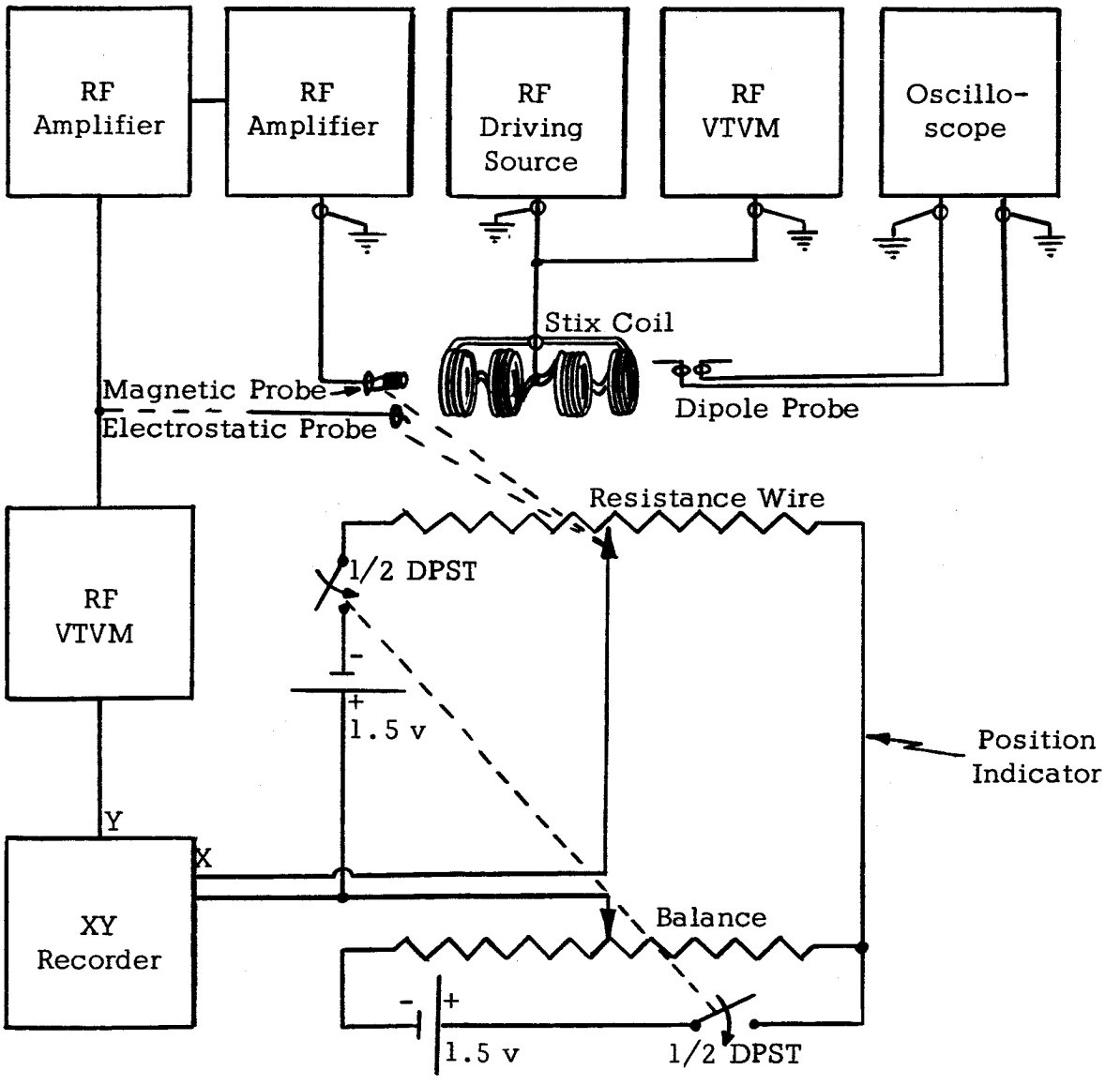

Fig. IV-2 Schematic of Probe Position Indicator and Block Diagram of Diagnostic Equipment

checked and calibrated, and has shown excellent repeatability and linearity in all cases.

The coil pickup signal is amplified by two rf amplifiers, a Hewlett-Packard 460 AR, and an H.P. 460 BR, connected in cascade, providing a variable gain of between 0 and 20 db. The signal is then fed into a Hewlett-Packard 411 A rf voltmeter, with frequency range to 500 MHz, which further amplifies the signal. This meter provides a dc output, proportional to the ac signal input, of 1 volt peak for full deflection of the meter on any scale. This output is fed into the Y input of the X-Y recorder, providing an amplitude signal corresponding to $|\dot{B}_z|$ at the transducer location. The recorder is a Mosely 135 plotter which provides an 8 1/2" x 11" size plot of signal amplitude versus position.

A hand operated pully drive system provides the motive power for the transducer holder. Although the probe holder was originally hand propelled, the optical bench is not constructed for motion of the optical bench supports, and a jerkiness resulted which distorted the plots. The distortion was further enhanced by the rather long RC time-constant of the dc output circuit in the H.P. 411A, which was sometimes "behind" the actual decreases of the rf signal. The hand-crank system provides for exceptionally slow, smooth motion of the transducer through the Stix coil, and there have been no distortions of the plots using it.

The driving signal for the Stix coil is provided by an rf signal generator, which has been modified for an output frequency of 5.8 MHz (corresponding to the frequency of the RF unit on the main ICRH experiment). It is connected to the coil coaxial input by simple solder joints, there being no particular need to insure good impedance matching, since there are very low powers involved. The driving unit delivers approximately 1.5 watts of rf power to the coil input, and the actual rms voltage at the coil itself (center-to-end) is about 6 v ac. This is sufficient to provide signal magnitudes useful with the present transducers. Input voltage to the coil is monitored through a second rf voltmeter.

The electrostatic pickup uses the same plotting system, except that the probe signal is fed directly into the H.P. 411A (bypassing the amplifiers)

(Fig. IV-2). Tests were run to verify that the conducting paper did not distort the fields in any noticeable way, a fact borne out by the test results with the "Aquadag" and conducting paper shields, as described further in the next section.

The dipole probe signal is fed directly into a Type W differential comparator on a Tektronix Model 555 oscilloscope. The display is then tabulated by hand or recorded on Polaroid film, using an oscilloscope camera.

A gear operated plotting device (Fig. IV-3) was also constructed so that plots of $|\dot{B}_z|$ versus radial position could also be plotted. This was quite useful in verifying the approximation $\partial \dot{B}_z / \partial r \simeq 0$, which was assumed in the derivation of the $E_\theta - \dot{B}_z$ relation.

Due to the inherent "noisiness" of the coil arrangement, as experienced in early test work, all intercomponent rf wiring is completely shielded, using RG-58/U and RG-174 cable and BNC connectors. All diagnostic instruments are case grounded by use of the three-contact electrical power plugs.

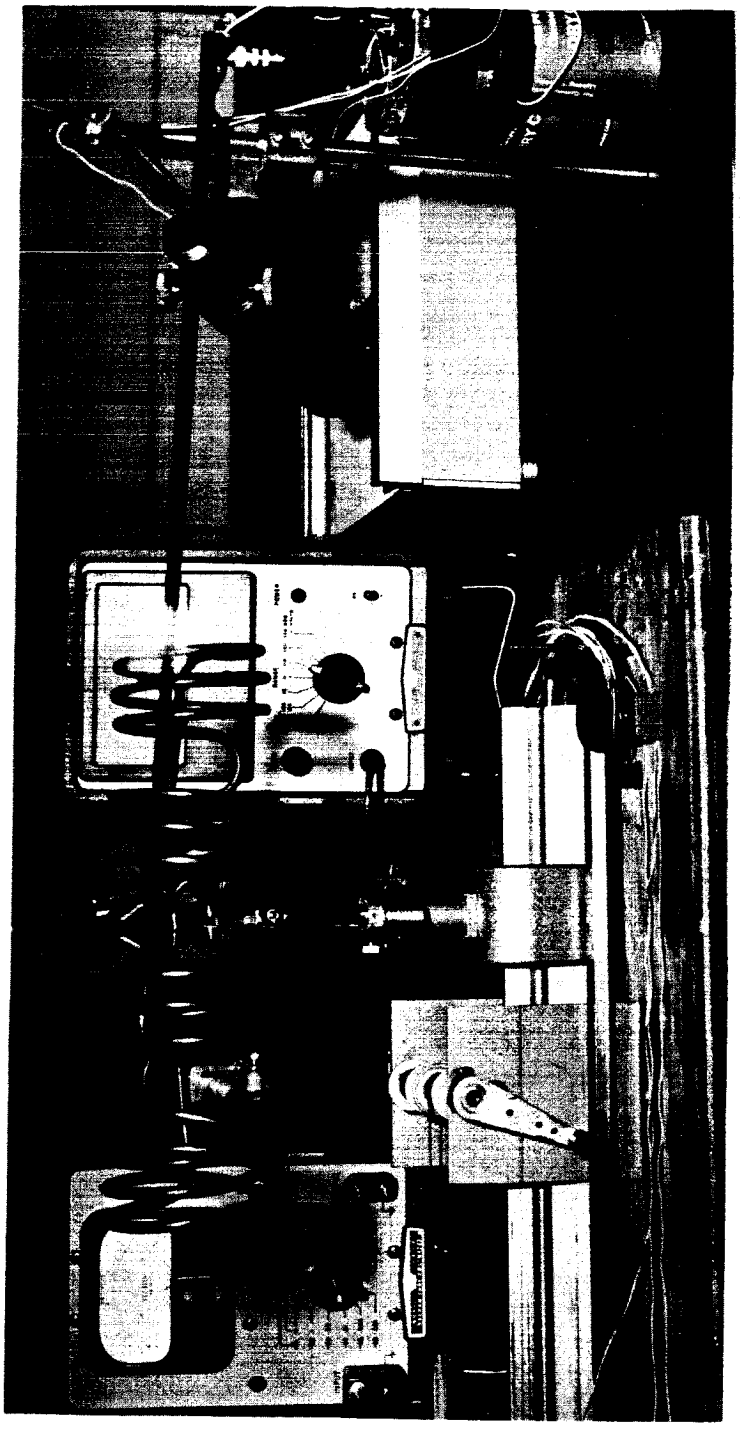

Fig. IV-3 Radial Probe Drive

CHAPTER V.

COIL AND SHIELD MEASUREMENTS

In the preliminary testing of the Faraday shields, the properties of shields S-5, S-6, and S-2 were found to be essentially similar, so that S-5 and S-6 were subsequently dropped from the investigation. Shields S-7 and S-8 were found to have negligible E_z shielding properties so that they were also dropped from further studies. The fact that these last two shields were ineffective was fortunate in that the resistive paper could then be used as a diagnostic tool with the electrostatic probe, as was discussed in Sec. III.

The remaining four types of shields were extensively evaluated with the various coils and their modifications. The results may be summarized in terms of the four basic topics which were investigated:

A. Shaping of the E_θ Field;

B. Effect of the Faraday Shields on E_θ Field;

C. E_z Shielding Efficiency of Faraday Shields; and,

D. Effect of Faraday Shields on Stix Coil Vacuum-Case Equivalent Circuit Parameters.

A. Shaping of the E_θ Field

As discussed previously, the E_θ waveform should theoretically be a pure sine wave two wavelengths long. Fig. V-1 is a drawing of the actual E_θ field for the 3-3-3-3 coil as shown in Fig. I-1b but with a pure sine wave imposed onto the trace for comparison. The effects are obvious, the outer two amplitude lobes of the Stix coil waveform being too high, and gradually decaying to zero outsize the Stix coil. Also, there is a very slight variation from the true sinusoidal along the leading and trailing slopes of the inner lobes, although this is practically negligible for a 3-3-3-3 coil. This last condition is more pronounced for a 1-1-1-1 coil, as may be seen from Fig. V-2. which compares the E_θ waveform for the 1-1-1-1 and 3-3-3-3 coils.

A solution to this last condition involves merely increasing the number

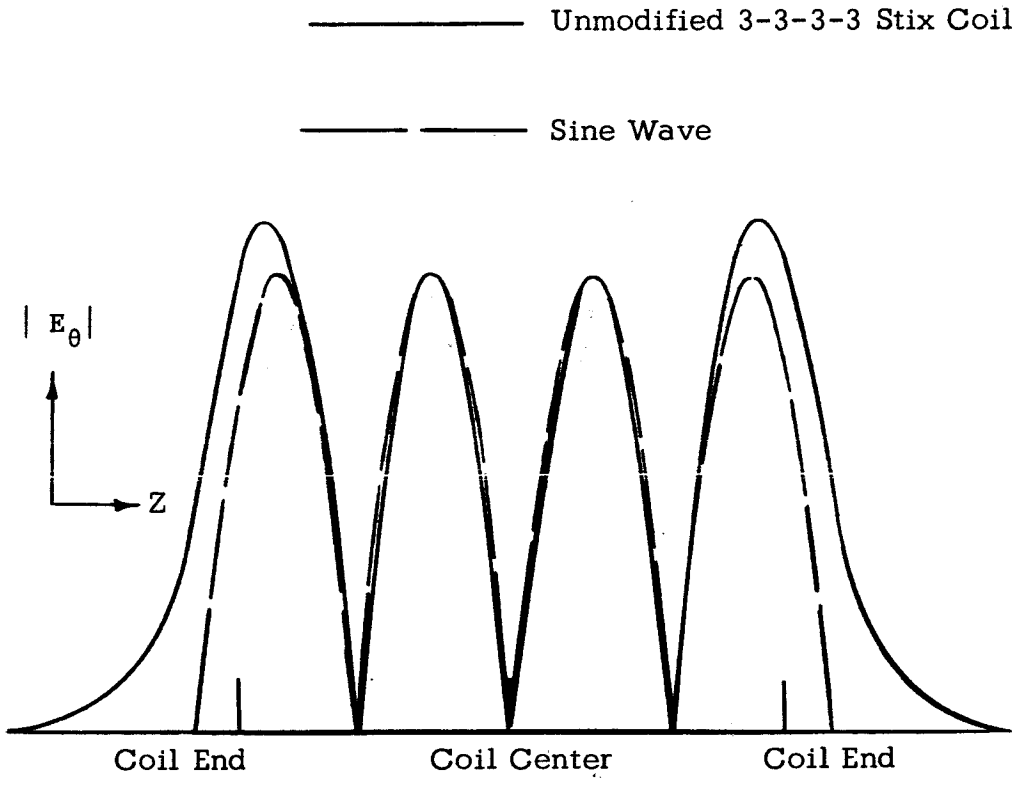

Fig. V-1 | E_θ | for Unmodified 3-3-3-3 Stix Coil with Plot of Pure Sine Wave Superimposed

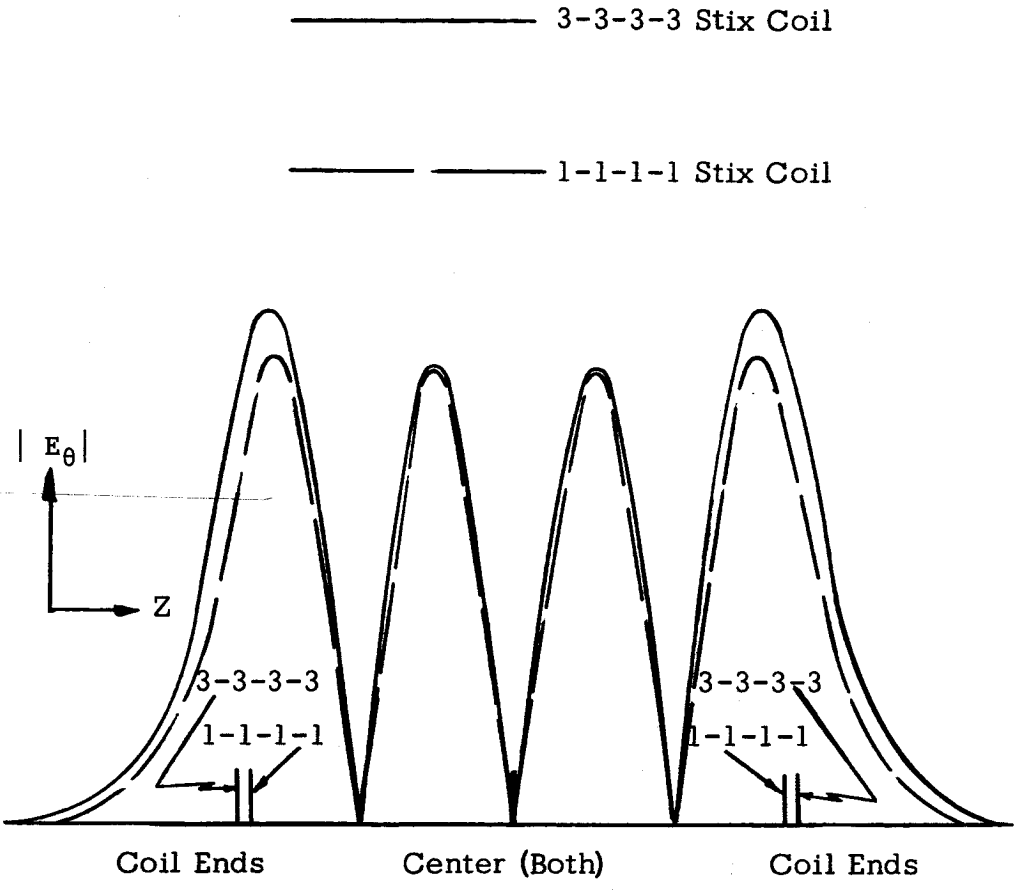

Fig. V-2 | E_θ | for Unmodified 3-3-3-3 and 1-1-1-1 Stix Coils

of turns in each section, as discussed in Section II. In order to determine the effect of this increase, a Fourier analysis of the 1-1-1-1 and 3-3-3-3 coil E_θ waveforms was performed. Several harmonics are introduced in each waveform, primarily the 1/2, 3/2 and 2nd harmonics. Surprisingly, however, the harmonic content of the 3-3-3-3 coil E_θ waveform is only slightly superior to the 1-1-1-1 coil waveform.

The reason may be inferred from a further study of Fig. V-2. Although the inner lobes of the 3-3-3-3 coil more closely approximate the true sinusoidal waveshape, the actual difference is small. But the significant distortions—the higher end lobes and gradually decaying waveform outside the coil—are substantially the same regardless of turn-per-section configuration, and it is these distortions, not the slight curvature variations of the sinusoidal parts of the curves, that produce most of the harmonic distortion. It can be seen that the "culprit" in the case of harmonic distortion is not fabricating error or inaccurate tolerances, but the end effects inherent in any coil of finite length, i.e., shorter than the plasma column.

To correct the amplitude variation, it was theorized that increasing the number of turns in the center coil sections would increase the E_θ amplitudes in these sections. Accordingly, a 3-4-4-3 coil was constructed, the E_θ waveform being shown in Fig. V-3. An overcompensation results with the inner lobes now too high, so that one distortion has been exchanged for another.

A second approach was to vary the turn spacing in the coil sections. The turns in the outer two sections of the 3-3-3-3 coil were spaced further apart, while the turns of the inner two sections were "squeezed" closer together, so that the turn spacing in the outer sections was approximately twice the spacing in the inner sections.

The result is shown in Fig. V-4. The amplitudes are identical in the four sections of the coil, but now a further distortion is introduced. The coil sections are now of different widths, so that the outer two lobes are considerably wider than the inner two lobes.

The last distortion was greatly reduced by the use of the shield S-3,

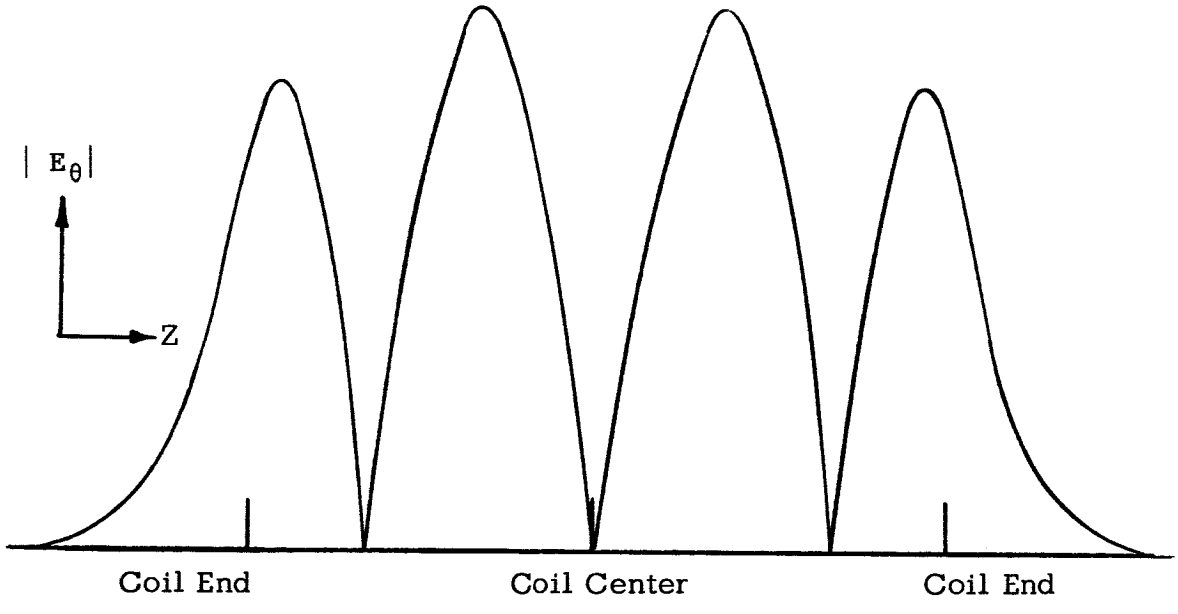

Fig. V-3 | E_θ | for 3-4-4-3 Stix Coil

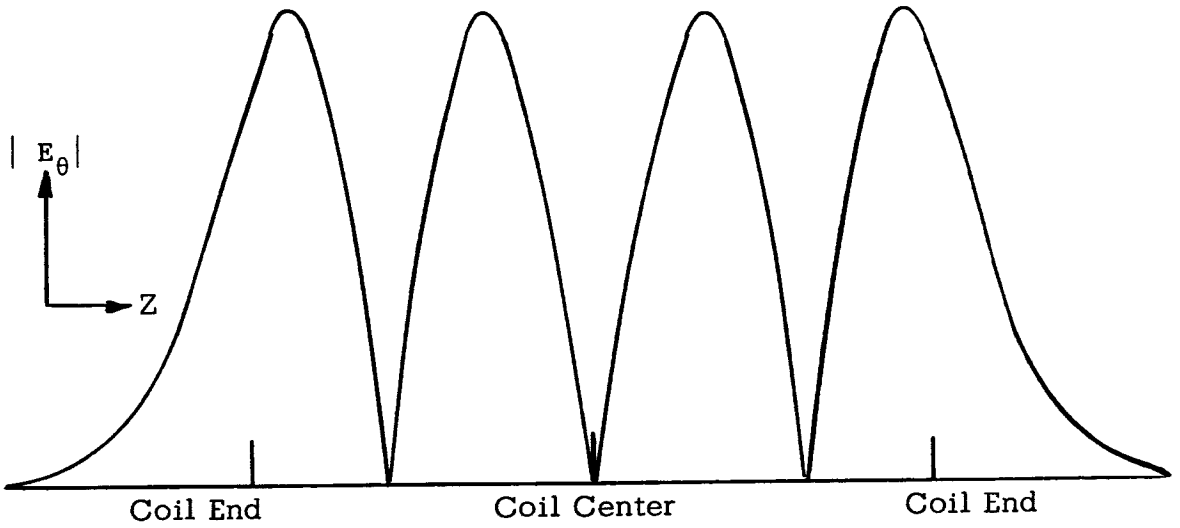

Fig. V-4 | E_θ | for Unshielded, Modified 3-3-3-3 Stix Coil

the "squirrel-cage" type shield. The shorting end straps at each end of this shield form nodes for the E_θ field, effectively shorting out and reducing the end effects, and narrowing the outer two lobes, as seen in Fig. V-5 which compares E_θ for the unshielded coil and with shield S-3. The resulting waveform was the closest approximation to a pure sine wave that was obtained. Fourier analysis of this waveform revealed that the excessive 1/2, 3/2 and 2nd harmonic content had been greatly reduced.

It might be noted that this reduction of the E_θ end effects is a "distortion" of the E_θ field, albeit a desirable one. The shorting effect due to the end straps causes some additional loading of the coil so that additional power is lost to the shield. But this additional loss must be minimal, as the maximum amplitudes are identical to the unshielded case.

B. Effect of the Faraday Shields on E_θ Field

Shield S-3 affects the E_θ field as described above, primarily shorting out undesirable end effects. However, no distortion or change of the actual waveform occurs, so that the shield does not appreciably reduce the coupling efficiency of the Stix coil.

Figure V-6 shows the E_θ waveform for the modified 3-3-3-3 coil with and without shield S-4. The results are similar to that for S-3, except that the outer amplitude lobes are lowered slightly, which tends to introduce greater harmonic content once again.

Figure V-7 depicts plots of E_θ for the modified Stix coil unshielded and with shields S-1 and S-2. Shield S-2 produces almost no effect at all on the E_θ field. However, shield S-1 causes a severe distortion of the E_θ field variation. The entire waveform is reduced in amplitude, and the inner two half-wavelengths are severly attenuated. The null points, or zeroes of the wave which should occur theoretically at 1/2 the wavelength and 3/2 the wavelength ($\lambda/2$ and $3\lambda/2$) are displaced.

A Fourier analysis of this distorted wave reveals that the fundamental is no longer the only major component. Approximately 60% of the signal appears in the fundamental, but most of the remaining 40% of the signal

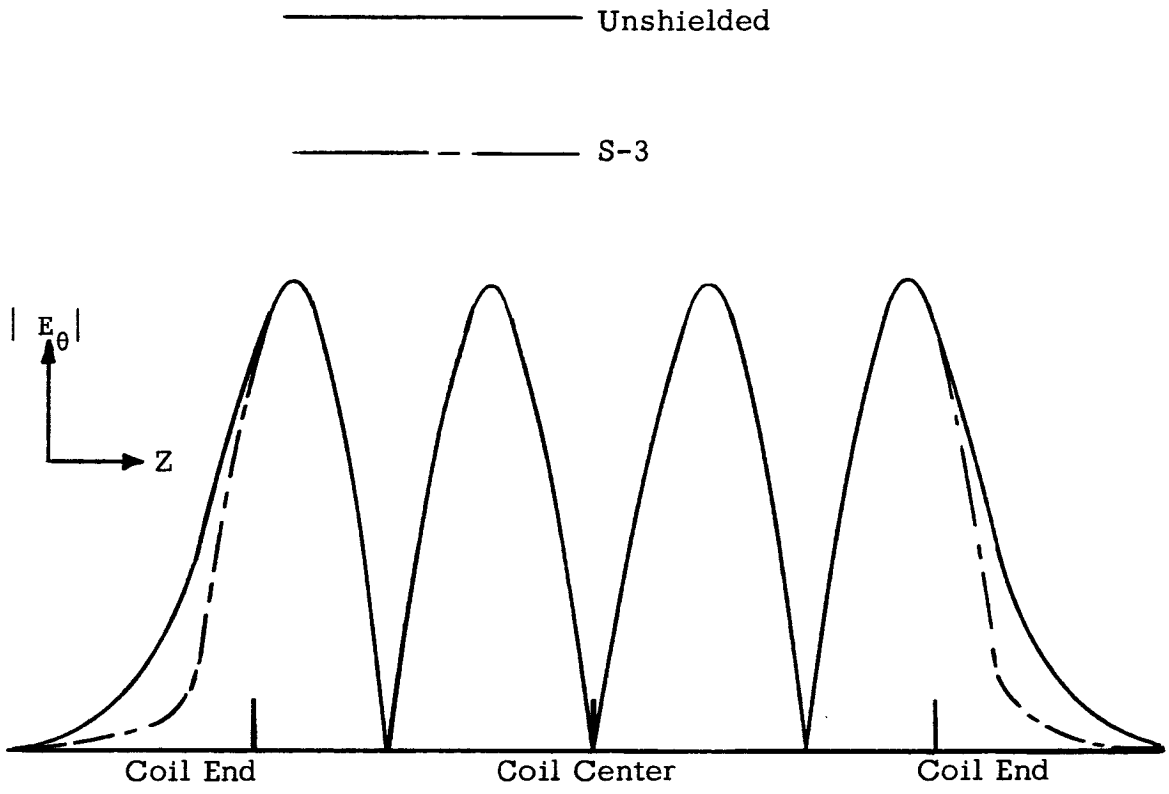

Fig. V-5 | E_θ | for Modified 3-3-3-3 Stix Coil Unshielded and With Faraday Shield S-3, Ungrounded

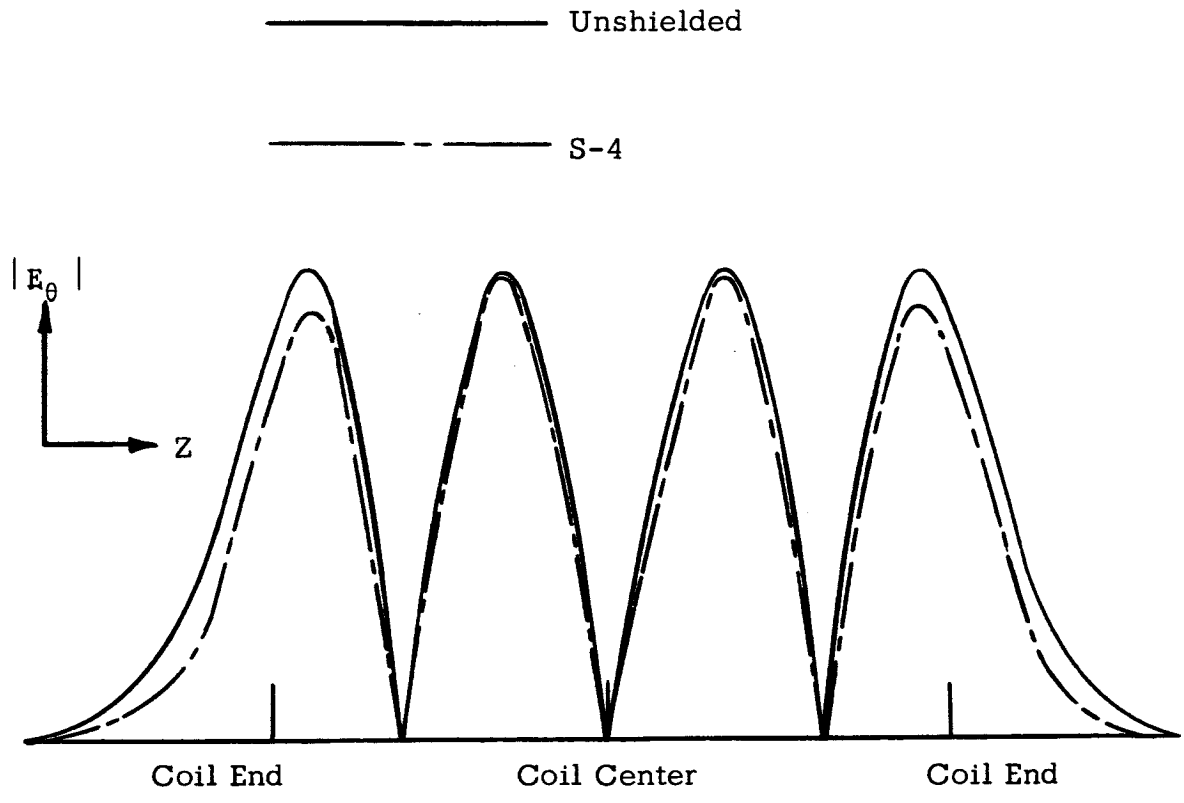

Fig. V-6 | E_θ | for Modified 3-3-3-3 Stix Coil Unshielded and With Faraday Shield S-4, Ungrounded

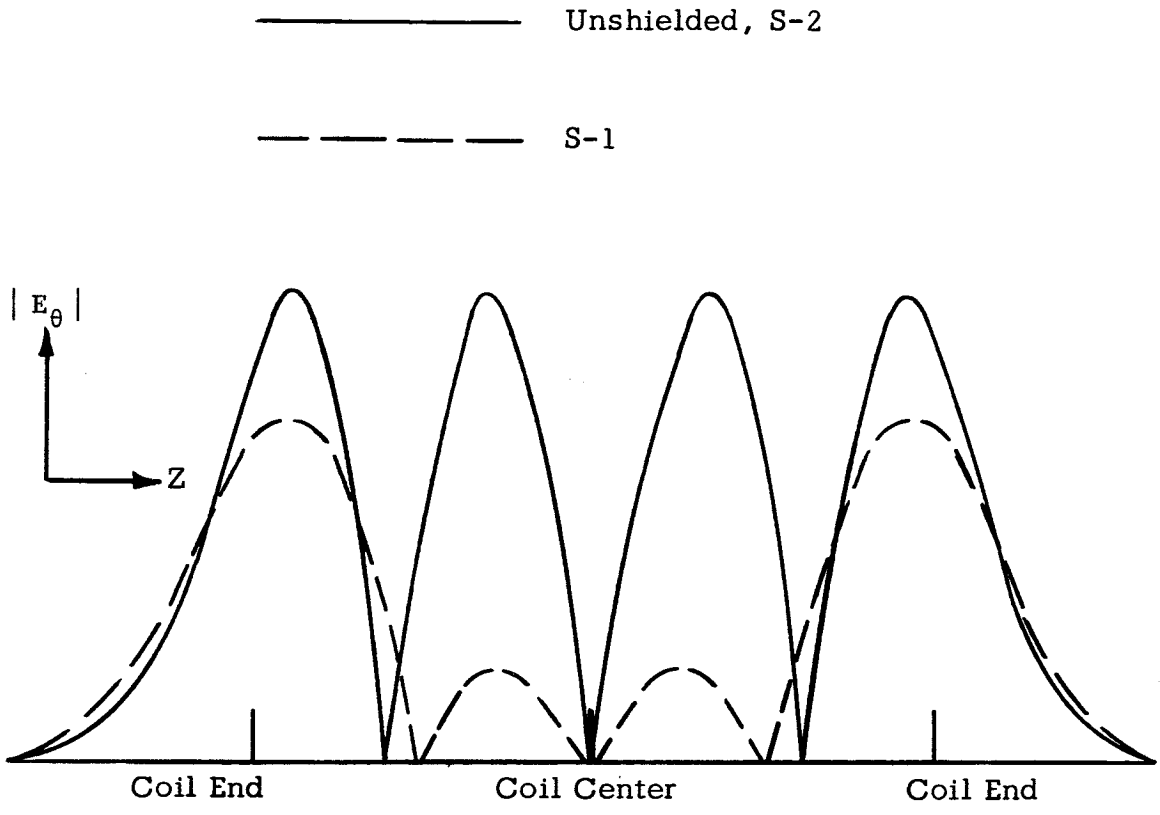

Fig. V-7 $|E_\theta|$ for Modified 3-3-3-3 Stix Coil Unshielded and With Faraday Shields S-1 and S-2, Ungrounded

appears at the first subharmonic ($=2\lambda$ in wavelength). There are two predominant waves now impressed upon the plasma, one with wavelength λ (or $\lambda + \delta$ where δ is some small increase due to the coil end effects), λ being the fundamental wavelength, and a second with wavelength 2λ (or $2\lambda + 2\delta$). This type of spatial variation has been previously reported[9] for a similar shield arrangement and provides correlation with the present work.

The question arises as to whether there is a distortion of the E_θ field or whether the single slit of shield S-1 introduces field asymmetries that void the approximation which relates E_θ and $\dot{B}_z$. The $E_\theta - \dot{B}_z$ relationship was derived in Sec. III from:

$$[\ \nabla \times \vec{E} = -\dot{\vec{B}}\ ]_z$$

or $(1/r)\partial(rE_\theta)/\partial r - (1/r)\partial E_r/\partial\theta = -\dot{B}_z$ (in cylindrical coordinates) where the E_r term $\rightarrow 0$ in the vacuum case. By suitable manipulation and integration by parts, the following relation was obtained:

$$E_\theta = (1/r)[\ (r^2/2)\dot{B}_z - \int_o^r (r'^2/2)(\partial\dot{B}_z/\partial r')dr'$$

and the condition for the approximate relationship was $\partial\dot{B}_z/\partial r \simeq 0$. Figure V-8 shows a typical radial plot of $\dot{B}_z$ for shield S-1 in the center region of the coil ($0 \leq r \leq r_{coil}/2$) and here $\dot{B}_z$ is nearly constant with respect to r. Thus, the approximation must hold in the center region of the coil where the plot of $\dot{B}_z$ (E_θ) was made for shield S-1 in Fig. V-7. The conclusion must be that the distortion of E_θ exists.

Grounding the shields was found to produce negligible effects on the E_θ waveform.

C. E_z Shielding Efficiency of Faraday Shields

The electrostatic probe was first used as a diagnostic tool for studying the shielding efficiency of the various Faraday shields. Although this method was more or less a "stop-gap" to supplement diagnostic procedures until the

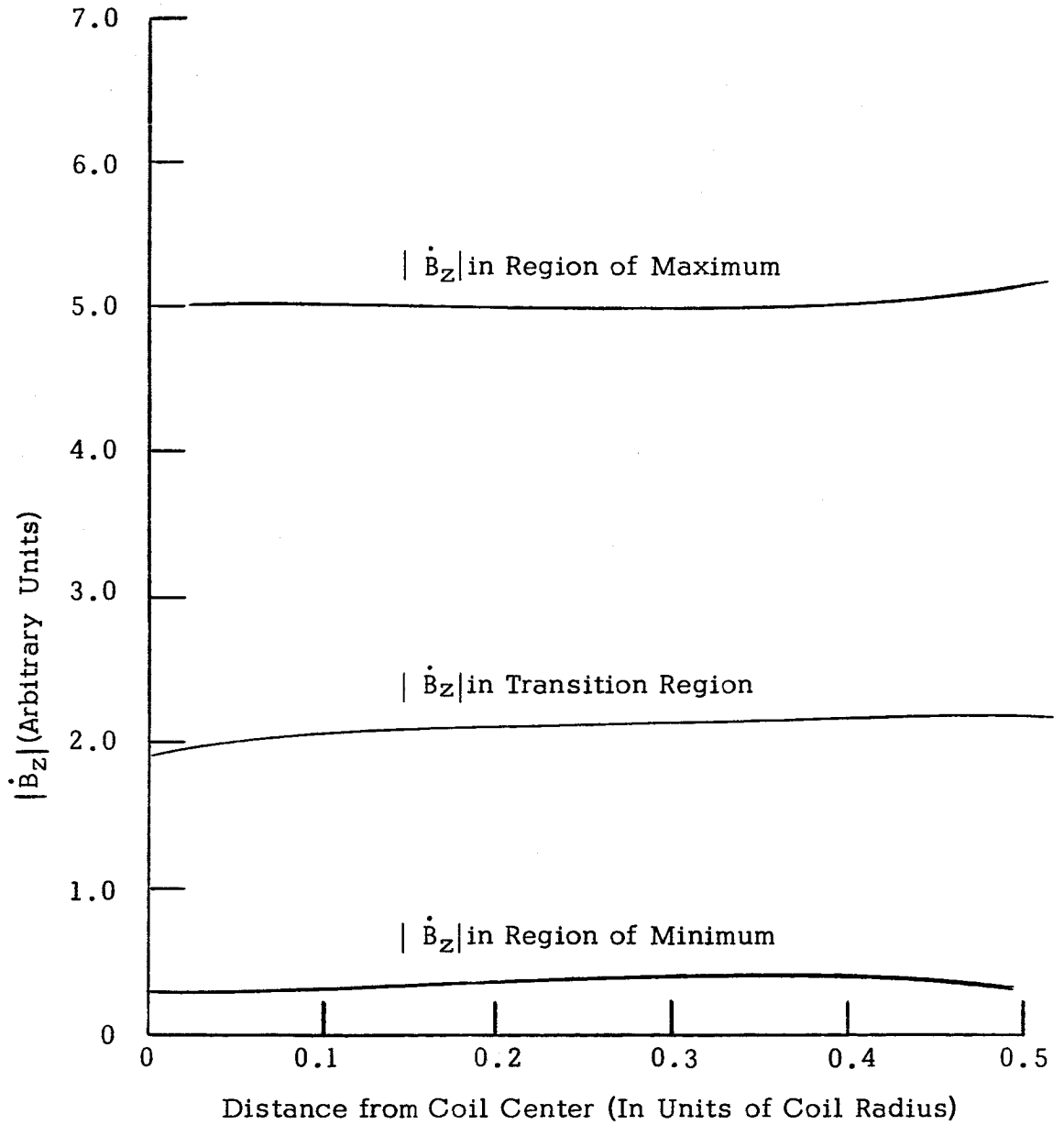

Fig. V-8 Radial Plot of $|\dot{B}_Z|$ in Center ($0 \leq r \leq r_{coil}/2$) of Stix Coil for Faraday Shield S-1

more sophisticated E_z dipole probe was devised, it produced results which correlate surprisingly well with the probe method.

Figure V-9 shows a plot obtained by running the electrostatic probe contact along the inner, graphite-coated surface of a tube of mylar insulated conducting paper, for the unshielded case and for shield S-3. What is recorded is the potential of the conducting paper, which is more or less uniform except for "noise" introduced by inhomogeneity in the graphite coating as the probe is moved along the paper surface. The reduction in tube potential is around 60% with shield S-3 in place, which, following the argument given in Sec. III, indicates around a 60% reduction in E_z. This is within about 20% of the reduction in E_z recorded by the dipole probe for shield S-3, and similar correlation was found in the cases of the other shields. The development of the E_z dipole probe pre-empted further use of the electrostatic probe, but the good correlation between the two methods provided additional verification of the theory involved.

The E_z dipole probe, because it utilized the oscilloscope and differential comparator, was not used with the electromechanical plotter developed for the E_θ and electrostatic probes. The amplitude display on the oscilloscope was hand-tabulated and then plotted. Such a plot is shown in Fig. V-10 for the unshielded E_z and for shields S-1, S-2, S-3, and S-4, ungrounded. The E_z field, unshielded, is quite asymmetrical near the inner coil diameter due to some small imperfections in the coil alignment, although these imperfections were subsequently improved by realignment of the coil. All shields reduce the E_z field to a uniformly low level, masking out large local E_z field variations. What is important here is not that E_z is only slightly reduced in certain places along the coil, but that the variation in E_z is kept at a low level and that variations, or local field perturbations due to flaws in construction, are "ironed out", or reduced to the same constant level. It is seen that such a sharp local peak in E_z as is shown in the figure might result in violent plasma interactions which would drive particles into the container, releasing impurities, and cooling the plasma.

The maximum value of E_z, shielded and unshielded, is the important

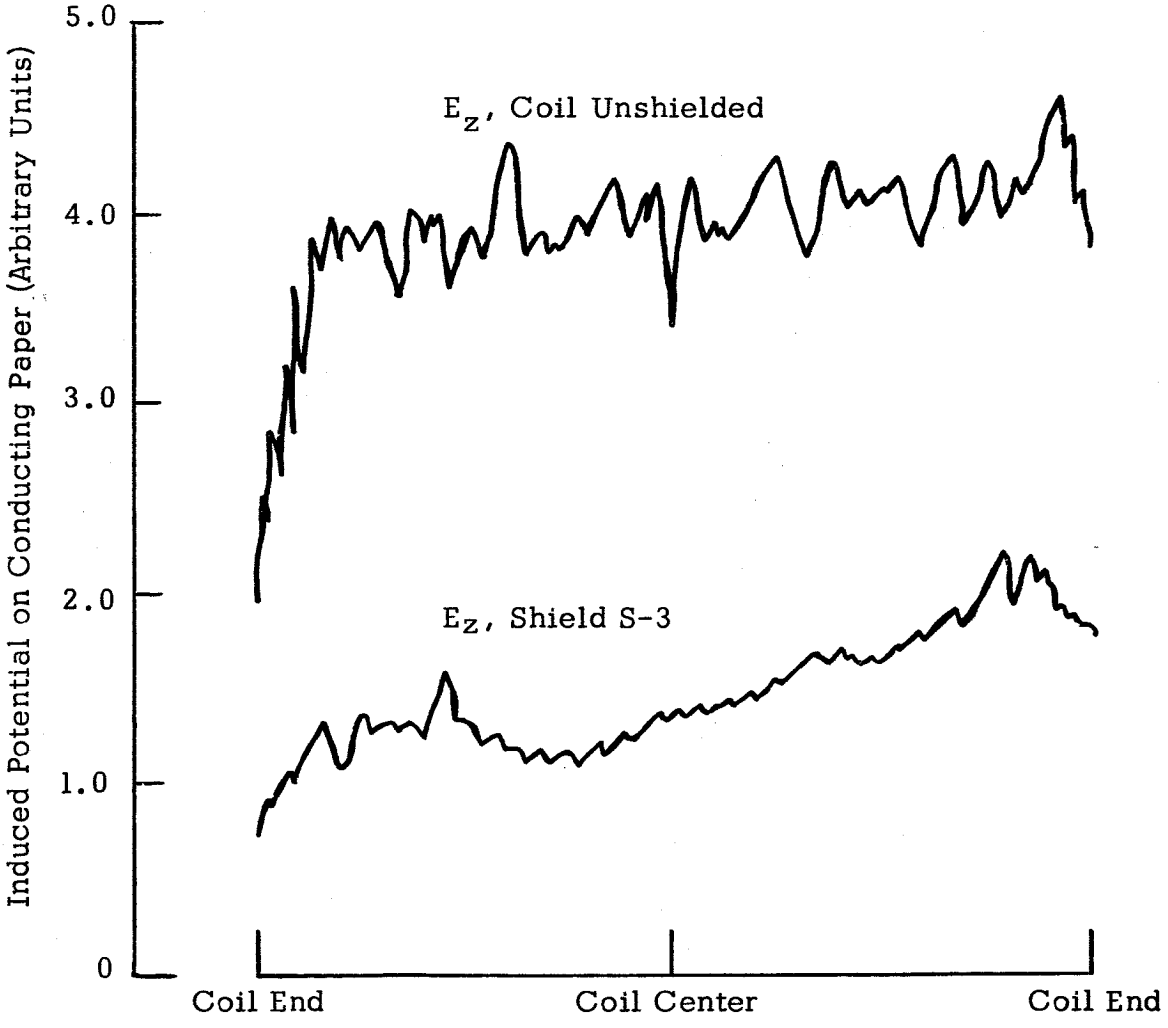

Fig. V-9 Electrostatic Probe Plot of 3-3-3-3 Modified Stix Coil Unshielded and With Faraday Shield S-3, Ungrounded

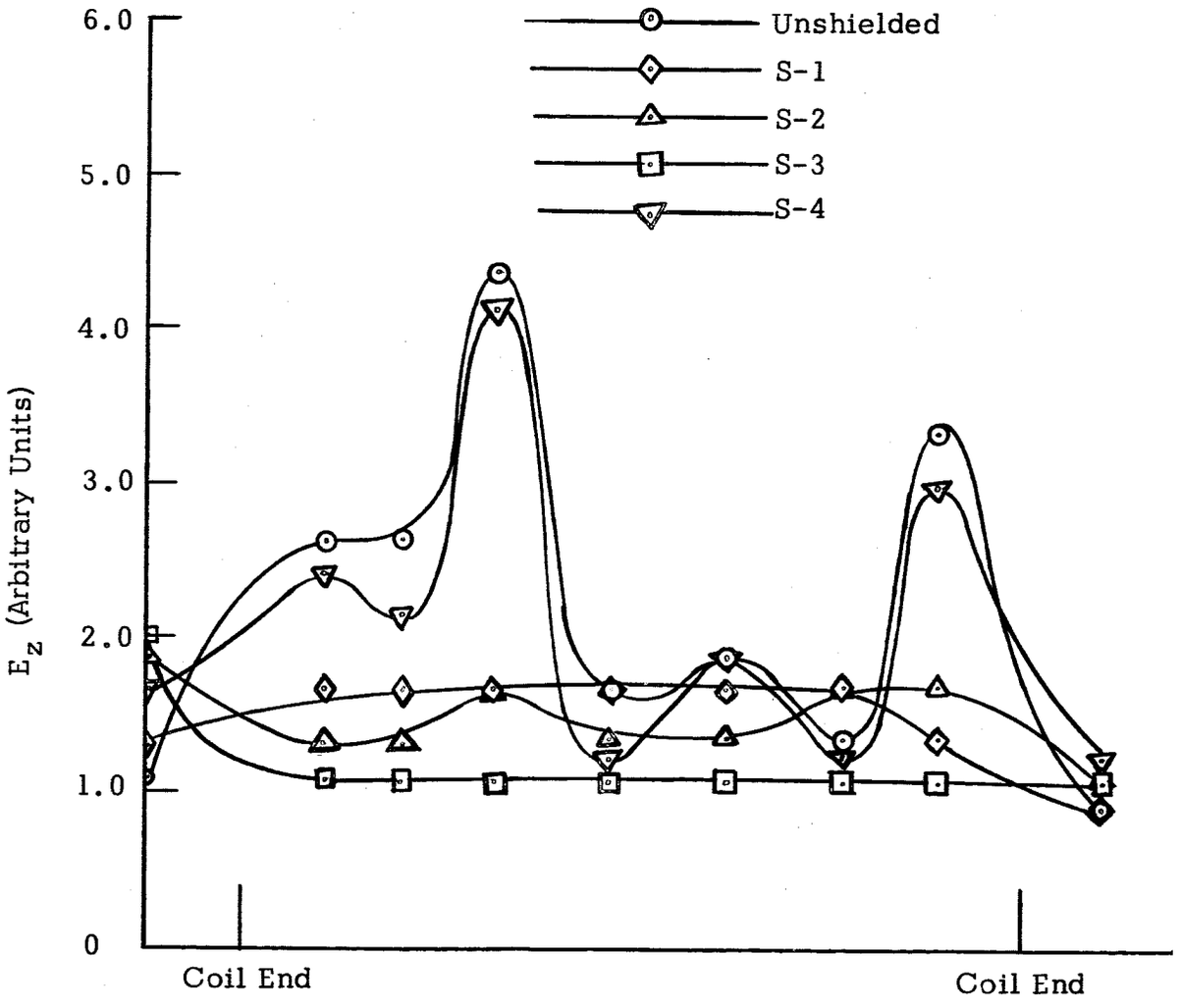

Fig. V-10 Plot of E_z for Modified 3-3-3-3 Stix Coil Unshielded and With Faraday Shields S-1, S-2, S-3, and S-4, Ungrounded

point. These values are tabulated below in Table V-1.

Table V-1

Maximum E_z For Unshielded 3-3-3-3 Coil and for Shields S-1, S-2, S-3, and S-4

Coil Condition	Max. Value of E_z (arb. units)
Unshielded	2.2
Shield S-1 ungrounded	0.8
Shield S-1 grounded	0.6
Shield S-2 ungrounded	0.8
Shield S-2 grounded	0.6
Shield S-3 ungrounded	0.6
Shield S-3 grounded	0.5
Shield S-4 ungrounded	2.1
Shield S-4 grounded	2.0

Shields S-1, S-2, and S-3 all were found to reduce the maximum E_z 60-80%, with shield S-3 being slightly superior. Grounding the shields uniformly improved the shielding about 5% in all cases, but normally resulted in severe loading of the coil and consequent reduction of the Q, as discussed below.

Shield S-4 reduced E_z very little and did not "flatten out" local E_z perturbations. Although the use of this type shield has been considered on certain experiments, it appears that such a shield is largely ineffective. The advantage of placing the shield between coil and plasma is clearly obvious.

D. Effect of Faraday Shields on Stix Coil Vacuum-Case Equivalent Circuit Parameters

A Boonton Model 160-A Q-meter was used in investigating the circuit parameters of the Stix coils. It was calibrated against a unit of known calibration with standard inductances. The circuit parameters were recorded, with and without shields at several frequencies of interest. Because of the low coil inductance ($\simeq 0.8$ μh) the Q meter could not tune the coil at exactly 5.8 MHz. However, data could be taken at 7.5 MHz, and although most of the parameters are frequency dependent to some extent, none fluctuate very

rapidly so that the data at 7.5 MHz can be taken as representative of the parameters at 5.8 MHz. Table V-2 summarizes the data for the ungrounded shields and the unshielded coil at 7.5 MHz.

Table V-2

Stix Coil Equivalent Circuit Parameters at 7.5 MHz (Shields Ungrounded)

Quantity	Unshielded	S-1	S-2	S-3	S-4
Coil Resistance (R_s) (Ω)	0.164	0.214	0.207	0.243	0.236
Coil Inductance (L_s) (μh)	0.822	0.624	0.848	0.866	0.885
Distributed Capacitance (C_d) (pf)	43.9	39.6	51.5	50.0	48.1
Q	236.	135.	179.	155.	162.

Grounding is desirable to reduce the fringing E_z field at the ends of the shield. But in all cases above, grounding the shields severely reduced the Q of the coil circuit and increased capacitance and effective resistance. These undesirable effects may be minimized by also grounding the ends of the Stix coil. Experimental investigation of ICRH at The University of Texas, however, has revealed that "floating" the Stix coil reduces some apparent plasma fluctuations and increases plasma heating.[12,13]

It is not clear why shield S-1 reduces the distributed coil capacitance while the others increase this quantity. Apparently the equivalent circuit for coil and shield involves both parallel and series capacitance terms, the series term predominating for the case of the solid shield and the parallel term predominating in the multi-strip shield case. The reduction in Q and increase in R_s verifies that there is some loading of the coil, as expected, even in the ungrounded case.

CHAPTER VI.

CONCLUSION

From results Sec. V-1, it is clear that the copper-tubing Stix coil may be modified easily to improve the shape of its accelerating field waveform. The "squirrel-cage" Faraday shield used with the modified coil gives further improvement of the shape of the E_θ field, while providing an E_z shielding efficiency as high as any of the shields tested.

The severe distortion of the accelerating field due to the single-slit, solid copper shield provides proof that a great deal of care in the design and use of Faraday shields is required. It is important to note that efficient shielding of the fringing E_z field is not sufficient reason for use, if the shield greatly distorts the accelerating field component. The resulting introduction of large spatial harmonics results in a wave which cannot transfer all of its energy efficiently to the particles in a plasma for one set of plasma parameters. Thus, the benefit of shielding results in a higher cost to the heating process.

Although shields S-2 and S-4 did not significantly alter the E_θ field, and shield S-2 provided satisfactory E_z shielding, the optimum condition is met only by shield S-3. Grounding in all cases increased the E_z shielding without substantially distorting the waveform, but here, the alteration of the Q and change of circuit parameters indicate that grounding produces a different tuning condition for the coil, so that efficient power transfer will be harder to obtain.

The Fourier analysis verifies that increasing the number of coil turns per section has limited importance, although an increase from one to three provides some slight reduction in spatial harmonic content of the wave. The prime causes of distortion are the end effects; the higher outer amplitude lobes and the gradual decay of E_θ outside the coil. These problems were met most successfully in this study by the variation of coil spacing in individual sections, and through the use of the ungrounded "squirrel-cage" shield, which also provided excellent shielding of the fringing E_z field while keeping additional loading of the Stix-coil circuit to a minimum.

The overall conclusion to be reached from this study goes a great deal further than the singling out of the "squirrel-cage" shield and individual turn-spacing on the Stix coil as the answer to energy coupling problems for ICRH at this facility. It shows that much needs to be done in the realm of energy coupling to the plasma, and that simple mechanical approaches are open with which to attack the problem. The Stix coil itself is only one of several energy couplers which have been proposed and used both here and abroad. These other approaches likewise must be considered so that more efficient means of ICRH may be attained. Some of these new methods of energy coupling, together with ideas gained from this study, are at present being pursued with this goal in mind.

At the same time, results of this study are being applied to the ICRH experiment at The University of Texas, making use of some of the concepts which have been more clearly defined herein. With this combination of results, leading to applications in the laboratory and stimulation of further research along the same lines, progress is being made in the continuing efforts of mankind to control thermonuclear fusion.

REFERENCES

1. T. H. Stix, "Generation and Thermalization of Plasma Waves", Phys. Fluids, 1, pp. 308-317, July-Aug., 1958.

2. A. G. Engelhardt and A. A. Dougal, "Dispersion of Ion Cyclotron Waves in Magnetoplasmas", Phys. Fluids, 5, pp. 29-37, Jan., 1962.

3. Y. J. Seto and A. A. Dougal, "The Wave Equation and the Green's Dyadic for Bounded Magnetoplasmas", J. Math. Phys., 5, pp. 1326-1334, Sept., 1964.

4. T. H. Stix, "Generation and Thermalization of Plasma Waves", Proceedings of the Second International Conference on Peaceful Uses of Atomic Energy, United Nations, Geneva, 31, pp. 125-133, (1958).

5. F. I. Boley, J. M. Wilcox, A. W. DeSilva, P. R. Forman, G. W. Hamilton, C. N. Watson-Munro, "Hydromagnetic Wave Propagation Near Ion Cyclotron Resonance", Phys. Fluids, 6, pp. 925-931, (1963).

6. M. P. Vasil'ev, L. I. Grigor'eva, V. V. Dolgopolov, B. I. Smerdov, K. N. Stepanov, and V. V. Chechkin, "Experimental Investigation of High-Frequency Energy Absorption in Plasma Near Ion Cyclotron Resonance", (Translated from report of the Fiziko-Tekhnicheskii Institut, Kharkov, 1963), Lawrence Radiation Laboratory Translation UCRL-Trans.-1167 (L).

7. E. S. Chambers, A. A. Garren, D. O. Kippenhan, W. A. S. Lamb, R. J. Riddell, Jr., "Cyclotron Resonance Heating of a Plasma in a Magnetic Mirror", U. S. Atomic Energy Commission Report UCRL-5286, USAEC TID 4500, June 17, 1958.

8. C. C. Swett, "Experiments on Inductive and Capacitive Radiofrequency Heating of a Hydrogen Plasma in a Magnetic Field", NASA Technical Note NASA TN D-2717, Lewis Research Center, Cleveland, March, 1965.

9. C. C. Swett, and R. Krawec, "Experiments on Ion-Cyclotron Wave Generation, Using an Electrostatically Shielded RF Coil", Bull. Am. Phys. Soc., 10, p. 509, April 26, 1965,
   Also,
   C. C. Swett, R. Krawec, G. M. Prok, and H. J. Hettel, "Experiments on Ion-Cyclotron-Wave Generation Using an Electrostatically-Shielded RF Coil", NASA Technical Memorandum NASA TMX-52091, Lewis Research Center, Cleveland, Preprint for American Physical Society Meeting, Washington, D. C., April 26-29, 1965.

10. M. Kristiansen, J. G. Melton, F. C. Harris, and A. A. Dougal, S.S.R. No. 4 on NASA Research Grant NsG-353, pp. 23-25, Jan. 15, 1965.

11. M. Kristiansen, J. G. Melton, F. C. Harris, N. B. Dodge, and A. A. Dougal, S.S.R. No. 6 on NASA Research Grant NsG-353, pp. 12-16, Jan. 15, 1966.

12. M. Kristiansen and A. A. Dougal, "High Power RF Plasma Heating and Wave Propagation Near the Ion Cyclotron Resonance Frequency", Proc. of Seventh Annual Meeting, Div. of Plasma Physics, Am. Phys. Soc., Nov. 8-11, 1965, Paper E5.

13. A. A. Dougal, M. Kristiansen, J. G. Melton, N. B. Dodge, F. C. Harris, Texas Biannual of Electronics Research No. 2, Laboratories for Electronics and Related Science Research, The University of Texas, pp. 127-132, Sept. 30, 1965.